

A Rationale for the Large Breathing of the Porous Aluminum Terephthalate (MIL-53) Upon Hydration

Thierry Loiseau,^{*[a]} Christian Serre,^[a] Clarisse Huguenard,^[b] Gerhard Fink,^[b] Francis Taulelle,^[b] Marc Henry,^[b] Thierry Bataille,^[c] and Gérard Férey^{*[a, d]}

Abstract: Aluminum 1,4-benzenedicarboxylate $\text{Al}(\text{OH})[\text{O}_2\text{C}-\text{C}_6\text{H}_4-\text{CO}_2]\cdot[\text{HO}_2\text{C}-\text{C}_6\text{H}_4-\text{CO}_2\text{H}]_{0.70}$ or MIL-53*as* (Al) has been hydrothermally synthesized by heating a mixture of aluminum nitrate, 1,4-benzenedicarboxylic acid, and water, for three days at 220 °C. Its 3D framework is built up of infinite *trans* chains of corner-sharing $\text{AlO}_4(\text{OH})_2$ octahedra. The chains are interconnected by the 1,4-benzenedicarboxylate groups, creating 1D rhombic-shaped tunnels. Disordered 1,4-benzenedicarboxylic acid molecules are trapped inside these tunnels. Their evacuation upon heating, between 275 and 420 °C, leads to a nanoporous open-framework (MIL-53*ht* (Al) or $\text{Al}(\text{OH})[\text{O}_2\text{C}-\text{C}_6\text{H}_4-\text{CO}_2]$) with empty pores of diameter 8.5 Å. This solid ex-

hibits a Langmuir surface area of 1590(1) m^2g^{-1} together with a remarkable thermal stability, since it starts to decompose only at 500 °C. At room temperature, the solid reversibly absorbs water in its tunnels, causing a very large breathing effect and shrinkage of the pores. Analysis of the hydration process by solid-state NMR (^1H , ^{13}C , ^{27}Al) has clearly indicated that the trapped water molecules interact with the carboxylate groups through hydrogen bonds, but do not affect the hy-

droxyl species bridging the aluminum atoms. The hydrogen bonds between water and the oxygen atoms of the framework are responsible for the contraction of the rhombic channels. The structures of the three forms have been determined by means of powder X-ray diffraction analysis. Crystal data for MIL-53*as* (Al) are as follows: orthorhombic system, *Pnma* (no. 62), $a = 17.129(2)$, $b = 6.628(1)$, $c = 12.182(1)$ Å; for MIL-53*ht* (Al), orthorhombic system, *Imma* (no. 74), $a = 6.608(1)$, $b = 16.675(3)$, $c = 12.813(2)$ Å; for MIL-53*lt* (Al), monoclinic system, *Cc* (no. 9), $a = 19.513(2)$, $b = 7.612(1)$, $c = 6.576(1)$ Å, $\beta = 104.24(1)^\circ$.

Keywords: aluminum · breathing effects · dynamic frameworks hydrothermal synthesis · nanostructures · structure elucidation

Introduction

There is currently considerable interest in the synthesis and characterization of hybrid organic-inorganic solids with infinite 1D-3D architectures.^[1] Beside metal-organic polymers,^[2-4] built up by the assembly of discrete metal (M) centers with functionalized organic ligands containing N- and/or O-donors, it has been shown that the dimensionality of the inorganic sub-network can be 1D or 2D,^[1,5] giving rise to original electronic, magnetic, or optical properties in addition to the usual zeolite-like^[6] ones (catalysis, gas separation, and, more recently, hydrogen storage^[7]). The apparent structural diversity observed for these topologies is often correlated with the atomic arrangements encountered in the basic structures of solid-state chemistry (diamond, quartz, rutile, and so on).^[8] Recently, searching for hybrid frameworks with 1D or 2D inorganic sub-networks, we focused our attention on the hydrothermal synthesis of dicarboxylates with various metals (rare earth elements^[9-12] and 3d transition metals^[13-16]), in particular using the well-known rigid linker

[a] Dr. T. Loiseau, Dr. C. Serre, Prof. Dr. G. Férey
Institut Lavoisier, UMR CNRS 8637
Université de Versailles St-Quentin en Yvelines
45 Avenue des Etats-Unis
78035 Versailles Cedex (France)
Fax: (+33)1-39-25-43-58
E-mail: loiseau@chimie.uvsq.fr

[b] Dr. C. Huguenard, Dr. G. Fink, F. Taulelle, Prof. Dr. M. Henry
Tectonique Moléculaire du Solide, UMR CNRS 7140
Université Louis Pasteur, Institut Le Bel
4 Rue Blaise Pascal, 67070 Strasbourg Cedex (France)

[c] Dr. T. Bataille
LCSIM UMR CNRS 6511
Cristallographie des Poudres et Réactivité des Solides
Université de Rennes I
Avenue du Général Leclerc, 35042 Rennes Cedex (France)

[d] Prof. Dr. G. Férey
Institut universitaire de France

1,4-benzenedicarboxylate (BDC), which has already been used to create several novel 3D architectures containing metallic clusters of zinc,^[17,18] copper,^[19] and rare earths.^[20] With trivalent metals such as vanadium(III) and chromium(III), two isotopic original porous hybrid frameworks, MIL-47^[21] and MIL-53^[22] were isolated, in which the connection of infinite *trans*-chains of M(III) octahedra with BDC entities generates one-dimensional rhombic channels. From the topological point of view, the occurrence of infinite M–O–M chains was new, since only discrete metal clusters had hitherto been observed in this class of solids. Moreover, under calcination/hydration, the chromium solid was seen to exhibit an unusually large amplitude of breathing (close to 5 Å), without changing its topology.^[22]

A combined XRD/NMR/modeling study conducted after the synthesis of the Al homologue provided an insight into the origin of the flexible behavior. Only a few contributions have appeared in the literature for p elements.^[23–25] Herein, we report the first synthesis and structural characterization of the different forms of an aluminum dicarboxylate Al(OH)(BDC) isostructural to MIL-53,^[22] which exhibits unexpectedly high thermal stability. A combination of ²⁷Al, ¹³C, and ¹H NMR spectrometries has allowed analysis of the breathing effect that accompanies the hydration/dehydration processes. This has revealed that hydrogen-bonding interactions between water molecules trapped within the channels and the carboxylate groups of the BDC linkers are responsible for the dynamic switching of the structure.

Results and Discussion

Structure description: The three crystal forms of aluminum MIL-53 exhibit the same topology (Figure 1). The framework is built up by the interconnection of infinite *trans* chains of corner-sharing (via OH groups) AlO₄(OH)₂ octahedra by BDC ligands (Figure 2). Bond valence calculations,^[32] which generate values of 1.11 (*as*), 1.19 (*lt*), and 1.32 (*ht*), confirm the occurrence of a hydroxide anion on oxygen (2), required for the electroneutrality balance of the structure. The two carboxylate functions of each BDC anion are linked to two distinct adjacent aluminum cations. The interatomic distances are typical for Al–O in an octahedral surrounding (Al–O ≈ 1.82–2.00 Å) and for C–C and C–O of the BDC ligand (C–C ≈ 1.43–1.51, C=C ≈ 1.35–1.46, and C–O ≈ 1.39–1.23 Å). This connection mode in the framework generates 1D channels with different pore sizes depending of the nature of the inserted molecules, and it is these that are responsible for the large breathing effects.

In MIL-53*as* (Al), the tunnels (free dimensions 7.3 × 7.7 Å²) are occupied by disordered templating BDC molecules, present in their protonated form (see IR analysis). Their irreversible expulsion upon heating at 275 °C (see TG analysis) generates the high temperature form MIL-53*ht* (Al), which has empty pores. The channel dimensions become 8.5 × 8.5 Å². In spite of the hydrophobic character of the aromatic walls of the channels, the reversible adsorption of one water molecule per Al at room temperature gives rise to MIL-53*lt* (Al) and induces a significant modification

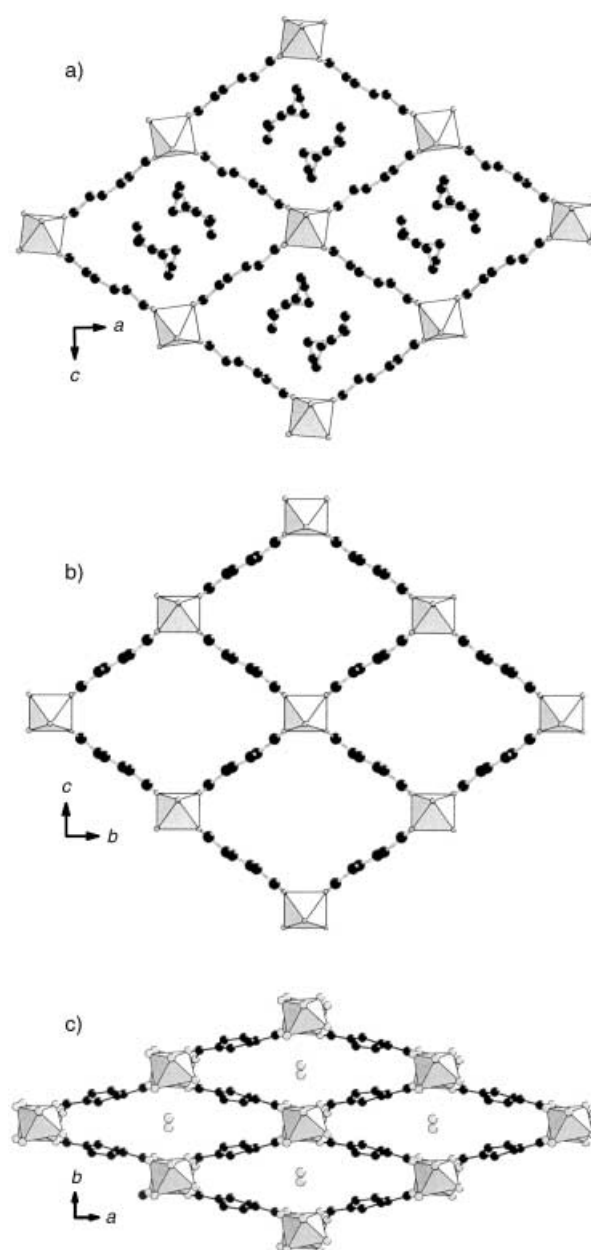


Figure 1. Views of the 3D structure of MIL-53 (Al) showing the channel system: a) Al(OH)[O₂C–C₆H₄–CO₂]_{0.70}·[HO₂C–C₆H₄–CO₂H]_{0.70} or MIL-53*as* (Al), in which the channels are occupied by free disordered 1,4-benzenedicarboxylic acid molecules; b) calcined form, MIL-53*ht* (Al) or Al(OH)[O₂C–C₆H₄–CO₂] with empty channels; c) room temperature form, MIL-53*lt* (Al) or Al(OH)[O₂C–C₆H₄–CO₂]_{0.70}·H₂O, in which a water molecule is located at the centre of the channels. Gray octahedra: AlO₄(OH)₂; black circles: carbon; gray circles: oxygen.

of the dimensions of the channels (2.6 × 13.6 Å²) through the establishment of a pair of hydrogen bonds between water and the hydrophilic part of the network (see NMR section). The two cell parameters affected by this modification vary from 16.675(3) × 12.813(2) Å² for the calcined form to 19.513(2) × 7.612(1) Å² for the hydrate. The final cell parameter, corresponding to the periodicity of the Al chains, remains almost identical in both cases.

Within the accuracy limits of powder data, the water molecule seems to preferentially interact with the oxygen atoms

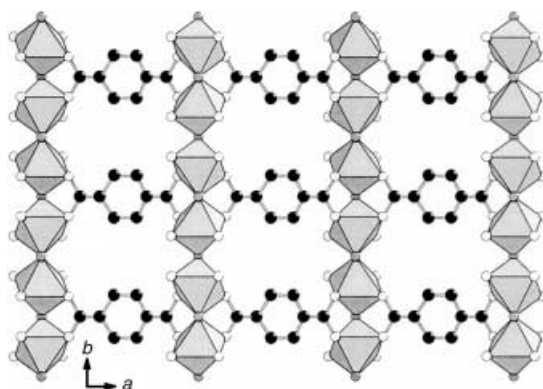


Figure 2. View of the infinite chains of corner-sharing octahedral $\text{AlO}_4(\text{OH})_2$ units connected through the 1,4-benzenedicarboxylate ligands; gray circles indicate the hydroxyl groups bridging the aluminum atoms.

of the carboxylate function ($\text{Ow}\cdots\text{O}(2) = 3.18(3)$, $\text{Ow}\cdots\text{O}(2b) = 2.92(4)$ Å) and the hydroxy group bridging the aluminum atoms ($\text{Ow}\cdots\text{O}(1) = 2.70(2)$ Å). However, without being able to locate the hydrogen atoms, it is difficult to establish the hydrogen-bonding scheme since there may also be some hydrogen-bonding interactions between the water molecules ($\text{Ow}\cdots\text{Ow} = 3.36(6)$ Å). This lack of information necessitated an NMR study to gain a better knowledge of the hydration and to rationalize the breathing effect.

Thermal behavior: The TG curve of MIL-53*as* (Al) (Figure 3a) shows two main events between room temperature and 700°C. As previously observed for MIL-53*as* (Cr),^[22] first the departure of the free disordered acid occurs in two steps within the range 275–420°C, with the observed total loss (36%) corresponding to 0.7 equivalents of BDC acid encapsulated within the pores. The first weight loss of 19% (0.37 BDC) induces the crystallization of an intermediate phase above 300°C (Figure 4), which disappears when the BDC molecules have been completely expelled (second loss of 17% (0.33 BDC) starting at 375°C). The second event, above 500°C, corresponds to the elimination of the BDC linkers from the framework. Between 500 and 600°C, MIL-53*as* is transformed into amorphous Al_2O_3 (obsd 47.8%; calcd 48.4%).

The thermal behavior of MIL-53*lt* (Al) is characterized by two weight losses (Figure 3b). The first (25–100°C) is assigned to the dehydration process, and corresponds to the removal of one equivalent of water molecules (obsd. 7.0%; calcd. 7.9%). The compound reversibly adsorbs and desorbs water in the ambient air. The dehydrated structure, which is stable up to 500°C, eventually collapses with the departure of the bound BDC acid (obsd 70.0%; calcd 70.2%). At 700°C, the final residue is again an amorphous form of Al_2O_3 .

A noticeable feature of MIL-53 (Al) is its remarkable thermal stability with respect to the vanadium^[21] or chromium^[22] analogues, which are only stable up to 350°C. Such a high decomposition temperature is quite unusual for this

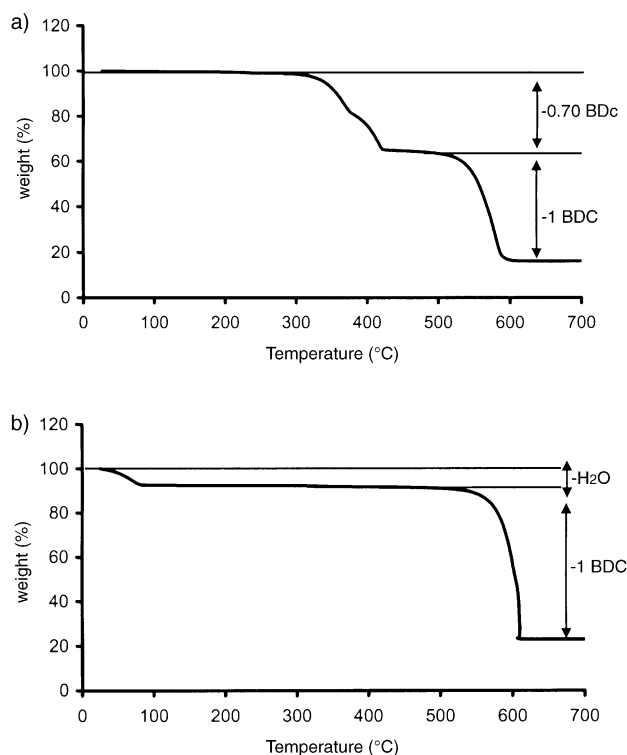


Figure 3. TG curves of a) MIL-53*as* (Al) and b) MIL-53*lt* (Al) in air (heating rate 5°C min^{-1}).

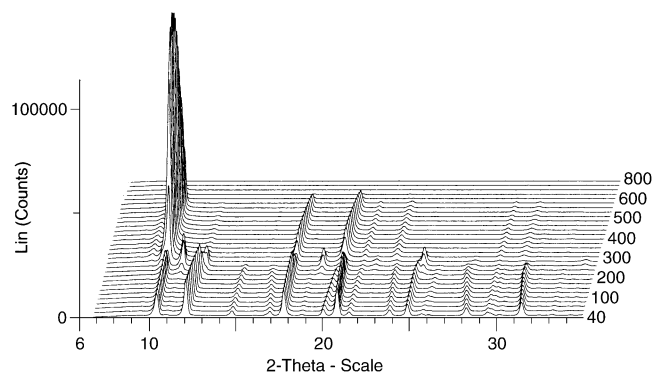


Figure 4. X-ray thermodiffractogram of MIL-53*as* (Al) in air (40–800°C). For clarity, a 2θ offset is applied for each pattern, which were collected at intervals of 20°C, except for the last two, which were collected 100°C apart.

class of solids, which are typically only stable below 400°C. Moreover, a nitrogen sorption experiment on MIL-53*lt* (Al) (degassed at 200°C overnight) revealed a type I isotherm without hysteresis upon desorption, which is characteristic of a microporous solid. The measured BET surface area is $1140(39)$ m^2g^{-1} and, assuming a monolayer coverage by nitrogen, the Langmuir surface area is $1590(1)$ m^2g^{-1} .

NMR study: The three forms, that is MIL-53*as* (Al), the calcined MIL-53*lt* (Al), and the monohydrate MIL-53*lt* (Al), were subjected to ^1H , ^{13}C , and ^{27}Al NMR measurements.

NMR characteristics of the three forms: The ^1H , ^{13}C , and ^{27}Al NMR spectra of MIL-53 *as*, *-ht*, and *-lt* are displayed in Figure 5. The samples of MIL-53 *as* and MIL-53 *lt* exhibit stable characteristics and the spectra do not evolve with time. In the ^1H spectrum (Figure 5c), the three signals at $\delta = 2.9$, 7.2, and 12.5 ppm can be assigned to the Al–OH–Al bridging hydroxides, the aromatic CHs, and the COOH groups, respectively.

Figure 5a,b display the ^{13}C NMR spectra. The signals between $\delta = 127$ and 136 ppm, attributable to the aromatic carbons, the CH units, and the quaternary carbons, are split due to the co-existence of the anionic form of the dicarboxylate of the framework and the acidic form present inside the pores. Signals in the region $\delta = 169$ –172 ppm can be assigned to the carbons of the carboxylic functions in both the protonated and deprotonated forms.

In the ^{27}Al NMR spectrum (Figure 5d), the single quadrupolar second-order pattern of MIL-53 *as* ($\delta_{\text{CS}} = 2.2$ ppm, a C_Q of 7.60 MHz, and a η_Q of 0.1) is flanked on its right-hand side as a shoulder with a broad line characteristic of amorphous $\text{Al}(\text{OH})_3$. As MIL-53 *as* is calcined, before degradation of the carboxylic acid molecules that occupy the pores, some of them may react with the slight excess of $\text{Al}(\text{OH})_3$ to form some additional MIL-53 *ht*. This is confirmed by the ^{27}Al NMR spectrum of the calcined form of MIL-53, which indicates no trace of any other aluminum-containing phase.

Study of the hydration: Figure 6a–d exhibit the series of $^{13}\text{C}\{^1\text{H}\text{-decoupled}\}$, $^{13}\text{C}\{^1\text{H}, \text{cross-polarized}\}$, ^1H , and ^{27}Al NMR spectra obtained on going from calcined (bottom) to fully hydrated samples (top). The two other sets of spectra represent intermediary steps of the hydration.

For the calcined sample, the ^1H NMR spectrum (Figure 6c) features two lines at $\delta = 1.7$ and 7.2 ppm attributable to the Al–OH–Al bridges and the aromatic CH, respectively. The $^{13}\text{C}\{^1\text{H}\text{-decoupled}\}$ spectrum (Figure 6a) features three lines at $\delta = 128$, 136, and 170 ppm. The latter two lines have about the same linewidths, and are much narrower than the CH signal at $\delta = 128$ ppm. The relative integrals of the signals at $\delta = 128$, 136, and 170 ppm are in the ratio 2:1:1, in agreement with their assignment. The $^{13}\text{C}\{^1\text{H}, \text{cross-polarized}\}$ spectrum (Figure 6b) is almost identical to the decoupled spectrum. This indicates a very strong localization of the hydrogen atoms and a good efficiency of polarization transfer. The ^{27}Al NMR spectrum exhibits a well-defined quadrupolar pattern with a chemical shift of $\delta = 3.3$, a C_Q of 8.36 MHz, and a η_Q of 0.

The ^1H NMR spectrum of the fully hydrated sample features three lines at $\delta = 1.7$, 4.5, and 7.2 ppm. The first is almost identical to that in the spectrum of the calcined compound. The signal at $\delta = 4.5$ ppm is clearly due to the presence of water in the structure. The poorly resolved signals at $\delta = 4.5$ and 7.2 ppm are much broader than that at $\delta = 7.2$ ppm in the spectrum of the anhydrous compound. In the $^{13}\text{C}\{^1\text{H}\text{-decoupled}\}$ spectrum, three lines are seen at $\delta = 128$, 136, and 174 ppm. The first two appear at the same chemical shifts as in the spectrum of the anhydrous sample, and can still be assigned to the aromatic CH and the aro-

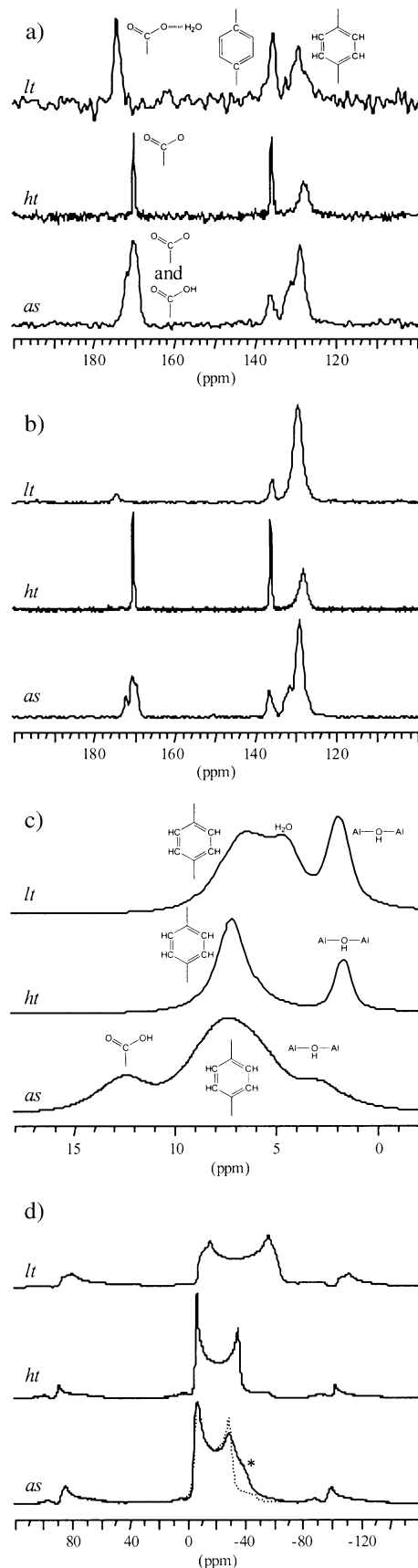


Figure 5. MAS NMR spectra of MIL-53 *as* (Al), MIL-53 *ht* (Al), and MIL-53 *lt* (Al): a) $^{13}\text{C}\{^1\text{H}\text{-decoupled}\}$; b) $^{13}\text{C}\{^1\text{H}\text{-cross-polarized}\}$; c) ^1H ; d) ^{27}Al , in which the MIL-53 *as* (Al) simulated component has been plotted in order to make clear that the line marked by with an asterisk corresponds to residual $\text{Al}(\text{OH})_3$ (see text).

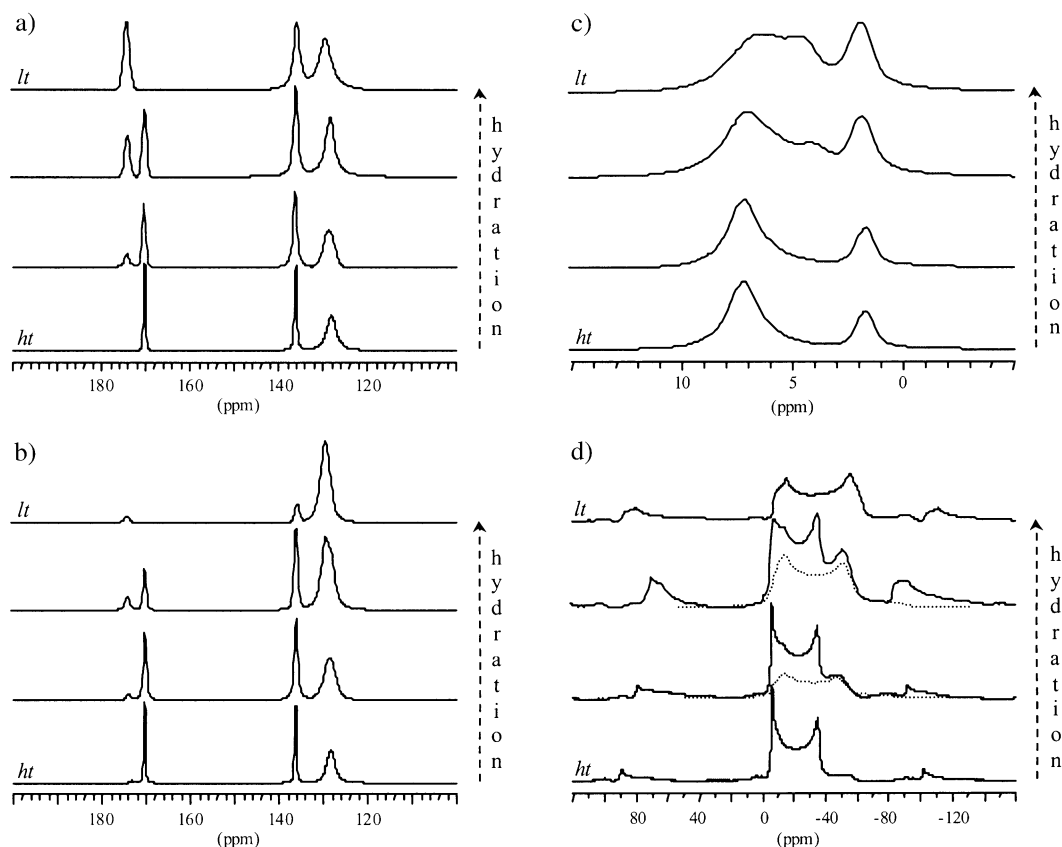


Figure 6. MAS NMR spectra of hydrating calcined MIL-53 (Al): a) ^{13}C $\{^1\text{H}$ -decoupled]; b) ^{13}C $\{^1\text{H}$ -cross-polarized]; c) ^1H ; d) ^{27}Al . From bottom to top for each series: first and second, spectra recorded after sample preparation according to Procedure 1 at $t = 0$ (*ht* form) and 45 min (approximately 30% hydrated, as can be roughly estimated from the spectra); third and fourth, spectra recorded after sample preparation accord-

ing to Procedure 2, at " $t = 0$ " (about 50% hydration has already occurred) and 2 h (*lt*, fully hydrated form). For the sake of clarity, the ^{13}C spectra plotted in this figure are simulations. In the ^{27}Al spectra of both intermediate hydrated states, the simulated component corresponding to the wet averaged structure is shown to indicate the dependence of the average quadrupolar interaction on the water content.

matic quaternary carbons, respectively. The line at $\delta = 174$ ppm is attributable to the carboxylic group under the influence of a water molecule. The $^{13}\text{C}\{^1\text{H}$, cross-polarized] spectrum exhibits a noticeable loss of intensity of the signal at $\delta = 174$ ppm. The two types of hydrogen atoms leading to cross-polarization are those of the CH units and those of the H_2O molecules. As the cross-polarization efficiency of the CH in the anhydrous compound proved to be sufficient to cross-polarize all the carbons, the loss of efficiency must be due to the additional, mobile water molecules. The ^{27}Al NMR spectrum exhibits a well-defined quadrupolar pattern with a chemical shift of $\delta = 3.4$ ppm, a C_Q of 10.67 MHz, and a η_Q of 0.15.

Analysis: The above observations concerning the three forms of MIL-53 (Al) are fully consistent with their respective structural analyses by XRD. However, the hydration process has unusual manifestations. Thus, while the ^1H NMR spectra show an increase in intensity of the water signal upon hydrolysis, both the CH and H_2O signals are displaced from their original positions, the latter showing an increase and the former showing a decrease in chemical shift, with a concomitant broadening of the lines. The Al–OH–Al signal shows a striking invariance with the increasing hydra-

tion state of the samples. The ^{13}C NMR spectra can be approximately viewed as being sums of contributions from the anhydrous and hydrated forms. The CP carbon spectra show a progressive decrease in intensity of the carboxylic signals. The ^{27}Al NMR spectra show a superposition of two lines, each with a quadrupolar pattern. One of these exhibits the same lineshape as seen for the anhydrous sample, while the second shows a continuous variation between the lineshapes seen for the anhydrous and hydrated samples. This continuously changing signal corresponds to the structure of the wet grains, being a static average between the signals due to dry open rhombic channels and the fully hydrated closed rhombic ones.

To rationalize these features, we attempted to localize the hydrogen atoms by applying the partial charges and hardnesses analysis method, PACHA.^[33,34] For a given geometry of atoms in a structure, the principle of PACHA relies on calculation of the partial charge on each atom, followed by an electrostatic energy calculation over periodic boundary conditions. Only the positions of hydrogen atoms are allowed to undergo a redistribution; all other atoms are fixed in the positions located in the diffraction analysis. The minimum energy obtained then corresponds to the best estimate for hydrogen atom localization. From this "static localiza-

tion" for the fully hydrated phase, some characteristics of the hydrogen atoms should be revealed.

In fact, for the MIL-53 case, two possible consistent structural models can be proposed on the basis of the PACHA calculations, and these are displayed in Figure 7 (the hydro-

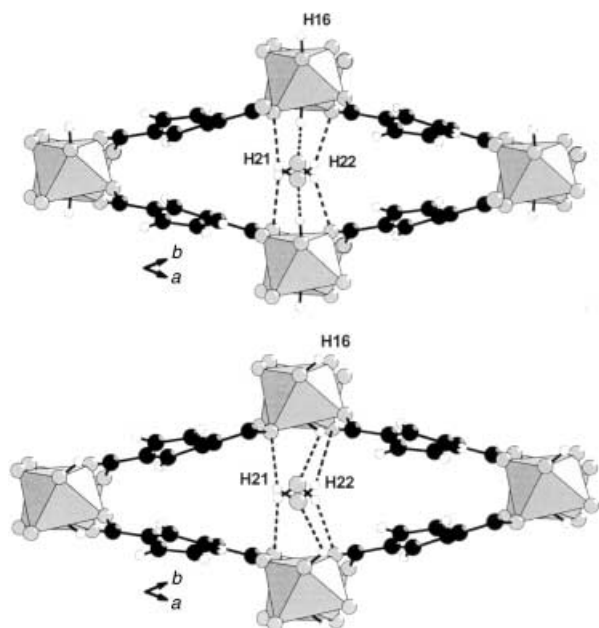


Figure 7. Hydrogen-bonding interactions between the occluded water molecule and the oxygen atoms of the MIL-53 network derived from PACHA calculations. Top: the hydrogen H16 of the hydroxyl group points towards the water molecule. Bottom: the hydrogen H16 of the hydroxyl group points towards the oxygen atoms of the carboxyl groups.

gen coordinates are provided as Supporting Information as an additional CIF file). Depending on the location of the hydrogen atom (H16) of the hydroxyl group, two situations may arise. Thus, this hydrogen H16 may be directed towards the water molecule and be involved in a strong hydrogen-bonding interaction ($O1-H16-Ow = 1.73 \text{ \AA}$), or it may be directed towards the oxygen of a carboxylic group. The latter case represents a weaker hydrogen-bonding interaction ($O1-H16-Ow = 2.33 \text{ \AA}$). In both situations, the hydrogen atoms of the water molecules interact preferentially with the oxygens of the carboxylic functions of the BDC linker ($Ow-H22 \cdots O2 = 2.31 \text{ \AA}$, $Ow-H21 \cdots O3b = 2.63 \text{ \AA}$, $Ow-H21 \cdots O2 = 2.63 \text{ \AA}$). The interatomic distances between the water molecules are much longer ($> 3.12 \text{ \AA}$) and prevent any significant hydrogen-bonding interactions along the channels (c axis). However, from the NMR results, it would seem that only the carboxylic groups are affected by the presence of occluded water within the pores. This observation would rule out the situation in which there is a strong hydrogen-bonding interaction between the bridging OH and the water molecules. It should be possible to confirm this specific point by either neutron diffraction analysis or NMR analysis, which would allow the positions of the hydrogen atoms in this structure to be determined. A study addressing this matter will be presented in the near future.

The above NMR results also provide information on the process involved during hydration. Indeed, some of the data show that the intermediate spectra are the sum of two contributions corresponding to the anhydrous and hydrated forms. This would imply that two types of crystallites coexist during the process, hereafter designated as "wet" or "dry" depending on their water content. If "dry" crystallites are present, they should give rise to the characteristic 1H , ^{13}C , and ^{27}Al spectra of the calcined form. This is indeed the case; in each spectrum one can discern the presence of a partial sub-spectrum characteristic of the "dry" crystallites. This does not hold for the "wet" crystallites: one cannot identify the sub-spectrum of the fully hydrated crystallites. For the "wet" crystallites, the water diffuses through the channels of the crystallites and gives rise to only one signal.

The NMR observations can now be rationalized. In the 1H spectra, the following situations may be observed. For the "dry" crystallites, two signals are seen, due to the Al-OH-Al and aromatic CH hydrogen atoms. For the "wet" crystallites, the Al-OH-Al signal remains unchanged (indicating that the hydroxides of the Al-OH-Al linkages are not affected by the water molecules), while the CH signals are shifted from their "dry" crystallite position. In the "wet" crystallites, a new H_2O signal is seen, which changes progressively as a result of an average water-framework interaction that is modified according to the amount of water. There is no exchange between "dry" and "wet" crystallites. The centers of gravity of both the "dry" and "wet" CH signals move towards lower chemical shifts, while the water signal moves towards higher chemical shifts.

Analyzing the ^{13}C NMR spectra, the aromatic signals are seen to be hardly influenced by the hydration, but the carboxyl group signals are distinctly affected, appearing at $\delta = 170$ and 174 for the "dry" and "wet" cases, respectively. The situation as regards the ^{27}Al NMR spectra is one of a fixed sub-spectrum due to the "dry" crystallites and a continuously varying component that depends on the water content, paralleling the continuous variation of the water signal seen in the 1H spectra. On increasing the amount of water, the water diffuses through the whole crystallite and gives rise to only one "wet" signal for all nuclei. In the 1H spectra, only the center of gravity of the CH signal of the "dry" and "wet" crystallites moves with the amount of water. In the ^{13}C spectra, there are only two signals, the "dry" and the "wet" signals showing minute variations in the chemical shift of the "wet" carboxyl group signals with the amount of water. As regards the ^{27}Al NMR spectra, the lineshape of the "wet" signal indicates a continuous second-order quadrupolar interaction, which can be attributed to the continuously varying structure according to the amount of water.

This diffusional exchange process is possible because of the dynamic flexibility of the framework.^[35] Indeed, coming back to the structure of MIL-53, it contains rigid parts, that is, the aromatic rings and, to a lesser extent, the chains of Al octahedra. However, owing to the contrasting natures of the Al-O and C-O bonds, the linkage between the octahedra and the carboxylic groups is flexible, and the linker can rotate about the O-O axis. Therefore, α , the BDC-Al-BDC angle, can vary within a large range, from

70.8° in MIL-53*as*, to 75.0° in MIL-53*ht* and 42.6° in MIL-53*lt*. Moreover, despite a significant rigidity, the octahedral chains have a certain degree of flexibility with various possibilities for tilting within the chains, specifically variation in the Al–OH–Al angle and the opposite rotation of two consecutive octahedra about the axis of the chain. Whereas the former is only slightly affected by the breathing effect (128.8°, 132.3°, and 129.0° for MIL-53*as*, *-ht*, and *-lt*, respectively), the rotation angle, which is zero for MIL-53*as* and *-ht*, reaches 20.3° after hydration.

When water enters the structure, the alternate rotation of aluminum octahedra begins to occur and propagates in the chains at the places in which the water is located owing to the creation of hydrogen bonds with the framework. These hydrogen bonds are also responsible for the contraction of the rhombic tunnels and the drastic decrease of the angle α from about 75° to 42°, thus providing a rationale for the breathing effect. As the water diffuses in the channels (along the *c*-axis) of the flexible framework, the net result observed is an “averaged” wet structure at intermediate levels of hydration between fully “dry” and fully hydrated. This averaged structure is well “sensed” by the quadrupolar interaction of aluminum, which provides a continuous measure of the constraint that water imposes on the structure.

Conclusion

The three forms of the aluminum 1,4-benzenedicarboxylate with the MIL-53 topology have been structurally characterized. MIL-53 (Al) belongs to the class of flexible networks,^[36] with water hydrogen bonding being responsible for the switching between the MIL-53*ht* and MIL-53*lt* forms. The very large breathing effect observed during hydration/dehydration has been explained in terms of the role of hydrogen-bonded water, as evidenced by a combined XRD/NMR/modeling study. These effects, previously reported for a metal organic network,^[36] have been analyzed, as is commonly the case, on the basis of the localization of the oxygen and nitrogen atoms.

As hydrogen-bonding is crucial to understanding the structural changes, further work in this direction will require accurate location of the hydrogen atoms by means of neutron diffraction or NMR analysis, or as we have done here with appropriate modeling. Such accurate hydrogen atom location can be expected to aid in the rationalization of many other known hydrogen-bonded networks.

Experimental Section

Synthesis: The synthesis was carried out under mild hydrothermal conditions using aluminum nitrate nonahydrate (Al(NO₃)₃·9H₂O, 98+%, Aldrich), 1,4-benzenedicarboxylic acid (C₆H₄-1,4-(CO₂H)₂ >98%, Merck, abbreviated as BDC hereafter), and deionized water. The reaction was performed in a 23 mL Teflon-lined stainless steel Parr bomb under autogenous pressure for three days at 220°C. The molar composition of the starting gels was 1 Al (1.30 g):0.5 BDC (0.288 g):80 H₂O. After filtering off and washing with deionized water, the resulting white product was first identified by powder X-ray diffraction analysis. It was found to con-

sist of a mixture of the as-synthesized MIL-53 (MIL-53*as* or Al(OH)-[O₂C–C₆H₄–CO₂]-[HO₂C–C₆H₄–CO₂H]_{0.70}) and unreacted BDC acid (easily identified by large needle-shaped crystallites). The solid was purified upon heating in air (330°C, 3 days). At this temperature, the unreacted BDC species and the occluded BDC molecules contained in the structure are expelled, thereby leading to MIL-53*ht* (Al) or Al(OH)-[O₂C–C₆H₄–CO₂]. After cooling to room temperature, the phase absorbs one equivalent of water molecules to give MIL-53*lt* (Al) (Al(OH)-[O₂C–C₆H₄–CO₂]-H₂O). Similar thermal behavior has been described for the chromium-based benzenedicarboxylate MIL-53 (Cr).^[22]

Infrared spectroscopy: IR spectra were recorded on a Nicolet 550 FTIR spectrometer at room temperature in the range 400–2000 cm⁻¹, with samples in potassium bromide pellets. The IR spectra (Figure 8a,b) of MIL-

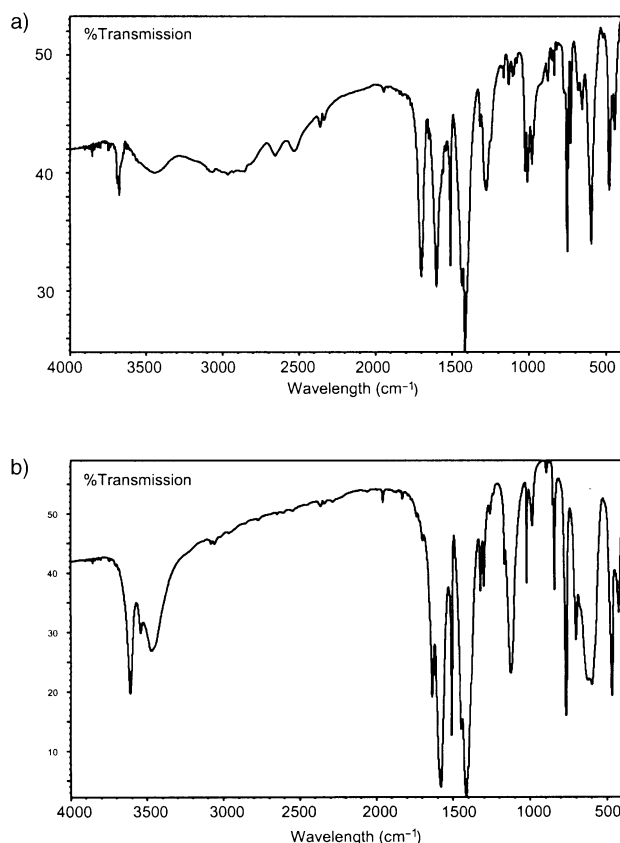


Figure 8. IR spectra of a) MIL-53*as* (Al), and b) MIL-53*lt* (Al).

53*as* (Al) and MIL-53*lt* (Al) exhibit vibrational bands in the usual region of 1400–1700 cm⁻¹ for the carboxylic function.^[26] For the as-synthesized material, two absorption bands, located at 1604 and 1503 cm⁻¹, can be assigned to -CO₂ asymmetric stretchings, whereas bands at 1435 and 1414 cm⁻¹ can be assigned to -CO₂ symmetric stretchings. These values are consistent with the presence of CO₂⁻ groups that are coordinated to aluminum. An additional absorption peak is observed at 1669 cm⁻¹, which can be attributed to molecules the free BDC acid that are encapsulated within the pores of the structure in their protonated form (-CO₂H). The IR spectrum of the hydrated form (MIL-53*lt*) is quite similar, except for the absence of an absorption band at around 1700 cm⁻¹. In this phase, free BDC molecules initially present within the pores but expelled upon heating have been replaced by water. The observed vibrational bands at 1632 cm⁻¹ and in the region 3600–3500 cm⁻¹ correspond to the bending and stretching modes of water, respectively. They also overlap with the signature of the hydroxyl group bridging the aluminum atoms.

Structure determination

X-ray powder diffraction: All attempts to obtain single crystals of MIL-53 (Al) were unsuccessful. Thus, the structures of the different phases

were determined on the basis of laboratory powder X-ray diffraction data. These were collected either on a Siemens D 5000 diffractometer (θ - 2θ mode, step size: 0.02° (2θ), time acquisition/step: 20 s) using $\text{Cu K}\alpha$ radiation ($\lambda = 1.5418 \text{ \AA}$) at room temperature (MIL-53*as* (Al) and MIL-53*lt* (Al)) or on a Siemens D 5005 diffractometer (θ - 2θ mode, step size: 0.02° (2θ), time acquisition/step: 50 s) equipped with an Anton Parr HTK 1200 high-temperature chamber at 275°C (MIL-53*ht* (Al)).

For MIL-53*as* (Al) and MIL-53*ht* (Al), the atomic coordinates of the chromium MIL-53 structural analogue^[22] were taken as a starting model for their structure determinations. For MIL-53*lt* (Cr),^[22] an anisotropic enlargement was observed for some reflections in its powder X-ray diffractogram, thus preventing any cell indexing and further structure determination analysis. No such peak enlargement was observed for the aluminum MIL-53*lt* (Al). Using the TREOR^[27] software, a monoclinic cell with satisfactory figures of merit was found for the aluminum form of MIL-53*lt*. The crystal parameters are as follows: $a = 19.513(2)$, $b = 7.612(1)$, $c = 6.576(1) \text{ \AA}$, $\beta = 104.24(1)^\circ$, and the structure may be described as belonging to the space groups $C2/c$ or Cc . The pattern-matching procedures were performed with Fullprof2k using the WinPLOTR software package.^[28,29] A direct calculation method, using EXPO,^[30] was applied to solve the structure of MIL-53*lt* (Al), while refinements of MIL-53*as* (Al) and MIL-53*ht* (Al) were based on the atomic coordinates of MIL-53*as* (Cr) and MIL-53*ht* (Cr), respectively. All the structures were refined using Fullprof2k. A small amount of unreacted 1,4-benzenedicarboxylic acid was found to be present, and this was refined as a secondary phase in the case of MIL-53*as* (Al). In the case of MIL-53*lt* (Al), the structure was refined first in $C2/c$ but a disorder was observed for the occluded water molecule; an ordering was observed when the structure was described in Cc , and hence the latter space group was chosen for the final refinements. Full details of the structure determination, including bond distances, are reported in the supporting information. The formulae deduced from the structure determinations of MIL-53*as* (Al), MIL-53*ht* (Al), and MIL-53*lt* (Al) are $\text{Al}(\text{O}-\text{H})[\text{O}_2\text{C}-\text{C}_6\text{H}_4-\text{CO}_2] \cdot [\text{HO}_2\text{C}-\text{C}_6\text{H}_4-\text{CO}_2\text{H}]_{0.70}$, $\text{Al}(\text{OH})[\text{O}_2\text{C}-\text{C}_6\text{H}_4-\text{CO}_2]$, and $\text{Al}(\text{OH})[\text{O}_2\text{C}-\text{C}_6\text{H}_4-\text{CO}_2] \cdot \text{H}_2\text{O}$, respectively. The final reliability factors^[31] (Table 1) are satisfactory. The corresponding Rietveld plots are shown in Figure 9. Atomic coordinates for the three forms of MIL-53 (Al) are given in Table 2.

Thermogravimetry: X-ray diffractometry was performed in the θ - θ mode in air with the sample in the furnace (Anton Paar HTK 16 high temperature chamber) of a Siemens D 5000 diffractometer (cobalt radiation). Each powder pattern was recorded in the 7 – 35° range (2θ) (at intervals of 20°C up to 600°C ; at intervals of 100°C up to 800°C) with a 2 s/step scan, corresponding to an approximate duration of 1 h. The temperature ramp between two patterns was 5°C min^{-1} .

Thermogravimetry: TG experiments were performed in air with a heating rate of 5°C min^{-1} using a TA Instrument TG 2050 apparatus.

Surface area study: The porosity of the dehydrated MIL-53*lt* (Al) was measured by means of a gas sorption isotherm experiment in liquid nitrogen using a Micromeritics ASAP 2010 apparatus (for surface area calculations, P/P_0 range: 0.01–0.3 (BET); 0.06–0.2 (Langmuir)).

Solid-state NMR spectroscopy: Solid-state ^{27}Al , ^{13}C , and ^1H NMR studies were performed on a Bruker DSX 500 spectrometer with a 11.7 Tesla magnetic field, in which these nuclei resonate at 130.3, 125.7, and

Table 2. Atomic coordinates for MIL-53 (Al).^[a]

atom	x/a	y/b	z/c
MIL-53 <i>as</i> (Al)			
Al	0	0	0
O(1)	0.000(2)	$-\frac{1}{4}$	$-0.071(1)$
O(2)	0.0867(9)	$-0.083(2)$	0.088(1)
O(3)	0.0650(9)	0.083(2)	$-0.110(1)$
C(1)	0.102(2)	$\frac{1}{4}$	$-0.130(3)$
C(2)	0.123(2)	$-\frac{1}{4}$	0.111(3)
C(3)	0.165(2)	$\frac{1}{4}$	$-0.207(3)$
C(4)	0.185(1)	$-\frac{1}{4}$	0.194(2)
C(5)	0.2312(9)	$-0.072(2)$	0.198(2)
C(6)	0.197(1)	0.074(2)	$-0.242(2)$
X(7a)*	0.014(3)	$-\frac{1}{4}$	0.309(2)
X(8a)*	0.140(3)	$-0.04(1)$	$-0.473(4)$
X(9a)*	0.138(3)	$-\frac{1}{4}$	0.447(4)
X(10a)*	0.131(2)	0.137(3)	0.459(2)
X(11a)*	$-0.025(2)$	$-\frac{1}{4}$	$-0.265(2)$
X(12a)*	0.046(1)	0.118(4)	0.374(2)
X(13a)*	0.085(2)	$-0.063(5)$	0.403(2)
X(14a)*	$-0.003(4)$	$-0.157(7)$	0.397(3)
MIL-53 <i>ht</i> (Al)			
Al	$\frac{1}{4}$	$\frac{1}{4}$	$\frac{3}{4}$
O(1)	0	$\frac{1}{4}$	0.693(1)
O(2)	0.156(1)	0.1670(4)	0.8417(6)
C(1)	$-0.192(1)$	0.0362(7)	0.974(1)
C(2)	0	0.060(1)	0.957(2)
C(3)	0	0.1292(9)	0.883(1)
MIL-53 <i>lt</i> (Al)			
Al	$-0.0012(8)$	0.000(2)	$-0.001(3)$
O(1)	$-0.000(2)$	$-0.110(1)$	0.744(5)
O(2)	0.0638(9)	0.173(3)	0.949(3)
O(2b)	$-0.0625(9)$	$-0.180(4)$	$-0.940(3)$
O(3)	0.0914(9)	0.099(2)	0.660(2)
O(3b)	$-0.0844(8)$	$-0.150(3)$	$-0.637(2)$
Ow	$-0.009(2)$	0.545(2)	0.830(6)
C(1)	0.1065(8)	0.179(6)	0.840(3)
C(1b)	$-0.1064(7)$	$-0.175(6)$	$-0.835(2)$
C(2)	0.2002(6)	$-0.277(4)$	0.629(2)
C(2b)	$-0.2036(8)$	0.242(4)	$-0.630(2)$
C(3)	0.2744(4)	$-0.300(6)$	0.719(2)
C(3b)	$-0.2754(8)$	0.299(6)	$-0.712(3)$
C(4)	0.1818(7)	$-0.211(5)$	0.422(3)
C(4b)	$-0.1796(5)$	0.228(5)	$-0.410(2)$

[a] *X = C or O.

Table 1. Crystal data for MIL-53*as* (Al), MIL-53*ht* (Al), and MIL-53*lt* (Al) or $\text{Al}(\text{OH})[\text{O}_2\text{C}-\text{C}_6\text{H}_4-\text{CO}_2] \cdot [\text{HO}_2\text{C}-\text{C}_6\text{H}_4-\text{CO}_2\text{H}]_{0.70}$, $\text{Al}(\text{OH})[\text{O}_2\text{C}-\text{C}_6\text{H}_4-\text{CO}_2]$ and $\text{Al}(\text{OH})[\text{O}_2\text{C}-\text{C}_6\text{H}_4-\text{CO}_2] \cdot \text{H}_2\text{O}$.

Formula	MIL-53 <i>as</i> (Al)	MIL-53 <i>ht</i> (Al)	MIL-53 <i>lt</i> (Al)
crystal system	orthorhombic	orthorhombic	monoclinic
space group	$Pnma$ (no. 62)	$Imma$ (no. 74)	Cc (no. 9)
a [\AA]	17.129(2)	6.6085(9)	19.513(2)
b [\AA]	6.6284(6)	16.675(3)	7.612(1)
c [\AA]	12.1816(8)	12.813(2)	6.576(1)
β [$^\circ$]			104.24(1)
number of reflections	219	256	179
R_p	10.6	13.7	11.4
R_{wp}	14.2	17.0	15.1
R_B	4.82	10.1	3.74

500.0 MHz, respectively. An H/X 4 mm MAS probehead and a classical ZrO_2 rotor spun at 12.5 kHz were used. For the acquisition of ^{27}Al MAS spectra, the RF field frequency, pulse duration, number of scans, and repetition time were 50 kHz, 1.5 μs , 8192 scans, and 400 ms, respectively. The corresponding parameters were 50 kHz, 5 μs , 32 scans, and 2 s for ^1H MAS spectra, and 50 kHz, 5 μs , 128 scans, and 4 s for ^{13}C MAS spectra with ^1H broadband decoupling, (referred to as $^{13}\text{C}\{^1\text{H}\text{-decoupled}\}$ in the text). For ^1H to ^{13}C CPMAS with ^1H broadband decoupling (referred to as $^{13}\text{C}\{^1\text{H}, \text{cross-polarized}\}$), we used 47.5 and 60 kHz RF field frequencies in the ^{13}C and ^1H channels, respectively, for CP. The contact time was 3 ms, and the repetition time was 2 s for 1024 scans. Chemical shift references (0 ppm) are $\text{Al}(\text{NO}_3)_3$ in aqueous nitric acid solution for ^{27}Al and TMS for ^1H and ^{13}C . NMR measurements were performed on the three forms of MIL-53 (Al), namely as-synthesized MIL-53*as*, the calcined MIL-53*ht*, and the hydrated MIL-53*lt*.

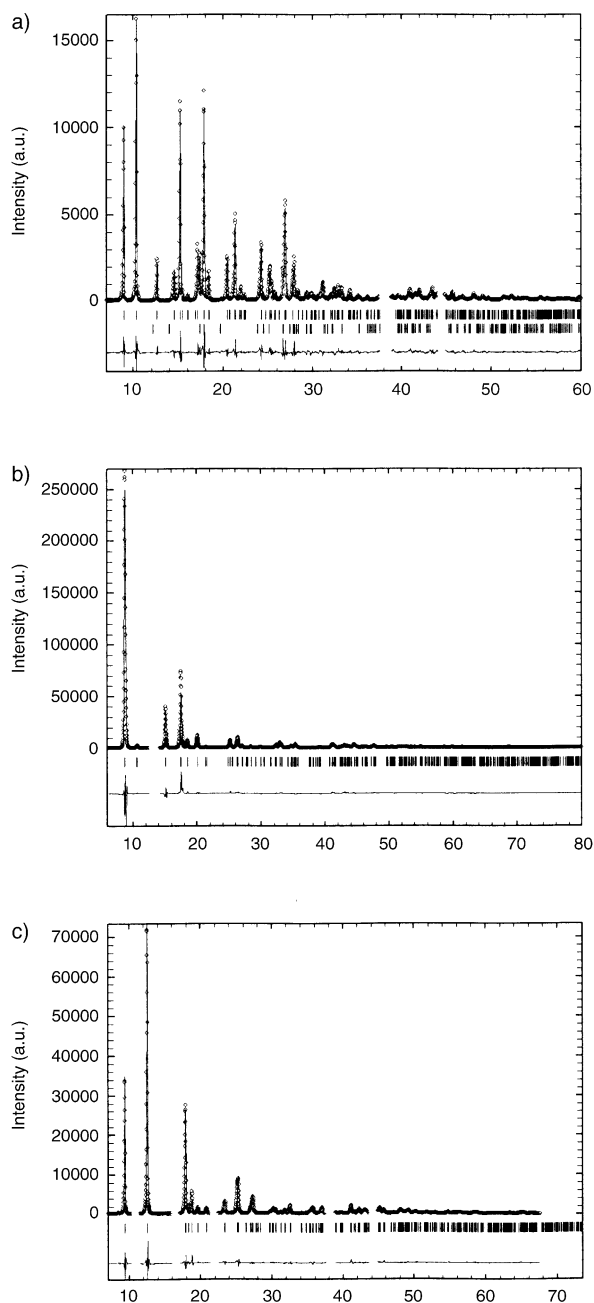


Figure 9. Final Rietveld plots of a) MIL-53*as* (Al); b) MIL-53*ht* (Al); c) MIL-53*ht* (Al). For MIL-53*as* (Al) powdered sample, a second minor phase (second row of vertical bars) corresponding to unreacted 1,4-benzenedicarboxylic acid was also refined together with MIL-53*as* (Al) (first row of vertical bars).

The hydration process of the MIL-53*ht* (Al) form was studied by room temperature NMR. No change in the hydration state of the sample in the closed rotor ever occurred during the measuring time necessary to study the series of nuclei. Two procedures for sample preparation were tested. Procedure 1 involved heating the MIL-53*ht* (Al) sample for four days at 140°C, followed by rapid transfer into a rotor, which was left open in the oven at 140°C for one day and then closed. In this way, a fully dehydrated sample could be obtained for NMR studies. The various hydrated states could subsequently be attained by allowing atmospheric water to diffuse into the open rotor for defined periods of time. In Procedure 2, the sample was simply enclosed in a rotor directly after dehydration in the oven. Thus, a significant amount of water was already present in the sample, leading to the occurrence of a very fast hydration process during

the 1–2 minutes necessary to fill the rotor with the powder in air. When following this procedure, different hydrated states were obtained by removing the sample from the rotor, dehydrating it once more in the oven, and allowing it to rehydrate in the surrounding atmosphere for chosen times before enclosing it again. In this way, after exposure to air for 2 h the hydrated sample was at equilibrium. Both sample preparation procedures led to fundamentally the same hydration process, as monitored by NMR, but with delayed kinetics and a more reproducible state when using Procedure 1.

CCDC-220475–CCDC-220477 contain the supplementary crystallographic data for this paper. These data can be obtained free of charge via www.ccdc.cam.ac.uk/conts/retrieving.html (or from the Cambridge Crystallographic Data Centre, 12, Union Road, Cambridge CB21EZ, UK; fax: (+44) 1223-336033; or deposit@ccdc.cam.ac.uk).

Acknowledgement

The authors are grateful to N. Katif, C. Thouvenot, and Prof. D. Riou (UVSQ) for their help in the synthesis work and fruitful discussions.

- [1] G. Férey, *Chem. Mater.* **2001**, *13*, 3084.
- [2] C. Janiak, *Angew. Chem.* **1997**, *109*, 1499; *Angew. Chem. Int. Ed. Engl.* **1997**, *36*, 1431.
- [3] B. Moulton, M. J. Zaworotko, *Chem. Rev.* **2001**, *101*, 1629; S. R. Batten, R. Robson, *Angew. Chem.* **1998**, *110*, 1558; *Angew. Chem. Int. Ed.* **1998**, *37*, 1460; M. Kondo, M. Shimamura, S.-I. Noro, S. Minakoshi, A. Asami, K. Seki, S. Kitagawa, *Chem. Mater.* **2000**, *12*, 1288; L. Carlucci, N. Cozzi, G. Ciani, M. Moret, D. M. Proserpio, S. Rizzato, *Chem. Commun.* **2002**, 1354; A. J. Fletcher, E. J. Cussen, T. J. Prior, M. J. Rosseinsky, C. J. Kepert, K. M. Thomas, *J. Am. Chem. Soc.* **2001**, *123*, 10001; E. J. Cussen, J. B. Claridge, M. J. Rosseinsky, C. J. Keper, *J. Am. Chem. Soc.* **2002**, *124*, 9574.
- [4] M. Eddaoudi, D. B. Moler, H. Li, B. Chen, T. M. Reineke, M. O'Keeffe, O. M. Yaghi, *Acc. Chem. Res.* **2001**, *34*, 319.
- [5] P. J. Hagrman, D. Hagrman, J. Zubieta, *Angew. Chem.* **1999**, *111*, 2798; *Angew. Chem. Int. Ed.* **1999**, *38*, 2638.
- [6] A. K. Cheetham, G. Férey, T. Loiseau, *Angew. Chem.* **1999**, *111*, 3466; *Angew. Chem. Int. Ed.* **1999**, *38*, 3268.
- [7] a) M. Eddaoudi, J. Kim, N. Rosi, D. Vodak, J. Wachter, M. O'Keeffe, O. M. Yaghi, *Science* **2002**, *295*, 469; b) N. L. Rosi, J. Eckert, M. Eddaoudi, D. T. Vodak, J. Kim, M. O'Keeffe, O. M. Yaghi, *Science* **2003**, *300*, 1127.
- [8] a) M. O'Keeffe, M. Eddaoudi, H. Li, T. Reineke, O. M. Yaghi, *J. Solid State Chem.* **2000**, *152*, 3; b) G. Férey, *J. Solid State Chem.* **2000**, *152*, 37.
- [9] F. Serpaggi, G. Férey, *J. Mater. Chem.* **1998**, *8*, 2737.
- [10] F. Serpaggi, G. Férey, *Microporous Mesoporous Mater.* **1999**, *32*, 311.
- [11] C. Serre, F. Millange, J. Marrot, G. Férey, *Chem. Mater.* **2002**, *14*, 2409.
- [12] C. Serre, G. Férey, *J. Mater. Chem.* **2002**, *12*, 3053.
- [13] C. Livage, C. Egger, M. Nogues, G. Férey, *J. Mater. Chem.* **1998**, *8*, 2743.
- [14] C. Livage, C. Egger, G. Férey, *Chem. Mater.* **2001**, *13*, 410.
- [15] M. Sanselme, J. M. Grenèche, M. Riou-Cavellec, G. Férey, *Chem. Commun.* **2002**, 2172.
- [16] N. Guillo, S. Pastre, C. Livage, G. Férey, *Chem. Commun.* **2002**, 2358.
- [17] H. Li, M. Eddaoudi, T. L. Groy, O. M. Yaghi, *J. Am. Chem. Soc.* **1998**, *120*, 8571.
- [18] H. Li, M. Eddaoudi, O. M. O'Keeffe, O. M. Yaghi, *Nature* **1999**, *402*, 276.
- [19] W. Mori, S. Takamizawa, *J. Solid State Chem.* **2000**, *152*, 120.
- [20] T. M. Reineke, M. Eddaoudi, M. O'Keeffe, O. M. Yaghi, *Angew. Chem.* **1999**, *111*, 2712; *Angew. Chem. Int. Ed.* **1999**, *38*, 2590.
- [21] K. Barthelet, J. Marrot, D. Riou, G. Férey, *Angew. Chem.* **2002**, *114*, 291; *Angew. Chem. Int. Ed.* **2002**, *41*, 281.

- [22] a) F. Millange, C. Serre, G. Férey, *Chem. Commun.* **2002**, 822; b) C. Serre, F. Millange, C. Thouvenot, M. Nogues, G. Marsolier, D. Louër, G. Férey, *J. Am. Chem. Soc.* **2002**, *124*, 13519.
- [23] C. C. Landry, N. Pappé, M. R. Mason, A. W. Apblett, A. N. Tyler, A. N. MacInnes, A. R. Barron, *J. Mater. Chem.* **1995**, *5*, 331.
- [24] R. Narayanan, R. M. Laine, *J. Mater. Chem.* **2000**, *10*, 2097.
- [25] B. Gomez-Lor, E. Gutiérrez-Puebla, M. Iglesias, M. A. Monge, C. Ruiz-Valero, N. Snejko, *Inorg. Chem.* **2002**, *41*, 2429.
- [26] K. Nakamoto, *Infrared and Raman Spectra of Inorganic and Coordination Compounds*, John Wiley, New York, **1986**.
- [27] P.-E. Werner, L. Eriksson, M. Westdahl, *J. Appl. Crystallogr.* **1985**, *18*, 367.
- [28] J. Rodríguez-Carvajal, Collected Abstracts of Powder Diffraction Meeting, Toulouse, France, **1990**, p. 127.
- [29] T. Roisnel, J. Rodríguez-Carvajal, WinPLOTR: A Windows tool for powder diffraction patterns analysis, *Materials Science Forum*, *Proceedings of the Seventh European Powder Diffraction Conference (EPDIC 7)*, Ed. R. Delhez and E. J. Mittenmeijer, **2000**, p. 118.
- [30] A. Altomare, M. C. Burla, M. Camalli, B. Carrozzini, G. L. Cascarano, C. Giacovazzo, A. G. Guagliardi, G. Polidori, R. Rizzi, *J. Appl. Crystallogr.* **1999**, *32*, 339.
- [31] R. A. Young, D. B. Wiles, *J. Appl. Crystallogr.* **1982**, *15*, 430.
- [32] N. E. Brese, M. O'Keeffe, *Acta Crystallogr. Sect. B* **1991**, *47*, 192.
- [33] M. Henry, *ChemPhysChem* **2002**, *3*, 561.
- [34] M. Henry, *ChemPhysChem* **2002**, *3*, 607.
- [35] G. Férey, submitted.
- [36] K. Uemura, S. Kitagawa, M. Kondo, K. Fukui, R. Kitaura, H.-C. Chang, T. Mizutani, *Chem. Eur. J.* **2002**, *8*, 3587.

Received: July 31, 2003

Revised: October 24, 2003 [F5413]